Volume 1 | Number 1 | Jan 2013 | Pages 1–100

PCCP

Physical Chemistry Chemical Physics
www.rsc.org/pccp

ROYAL SOCIETY OF CHEMISTRY

ROYAL SOCIETY OF CHEMISTRY

www.rsc.org/pccp

Exploration of the Presence of Bulk-like Water in AOT Reverse Micelles and Water-in-Oil Nanodroplets: Role of Charged Interface, Confinement Size and Water Properties

Vrushali R. Hande and Suman Chakrabarty[*]

Physical and Materials Chemistry Division, CSIR-National Chemical Laboratory, Pune-411008, India

KEYWORDS: Confined water, reverse micelle, water-in-oil, hydration layer, water structure and dynamics, tetrahedral order, reorientation dynamics

Corresponding Author

*s.chakrabarty@ncl.res.in

1

Abstract

The properties of water in a confined environment can be drastically different than the bulk water. In a confined system, e.g. interior of a reverse micelle, there exist at least two distinct regions namely "interfacial water" characterized by markedly slower dynamics, and "core water", which may resemble bulk water for larger size of the water pool. Using atomistic molecular dynamics simulations, we systematically investigate the presence of bulk-like water in AOT reverse micelles (RM) with varying size given by w_0 = [H_2O]/[AOT] = 10, 15 and 20. In order to understand the effect of the negatively charged interface of the RM, we have performed control studies for the model systems of water-in-oil (isooctane) nanodroplets with the same size of the water pool as the RM systems. In order to quantify the deviations from bulk-like behavior, we have used three kinds of structural order parameters, namely (i) number density to probe the local translational ordering, (ii) tetrahedral order and hydrogen bond distribution to probe the local orientational ordering, and (iii) dipolar orientation relative to the radial vector to capture the global orientational ordering of the water dipoles. We demonstrate that the size of the "core water" region that resembles bulk water decreases in the above order, i.e. orientational order parameters of water molecules are perturbed by the charged interface to a larger lengthscale as compared to the translational order. We have compared the translational and rotational dynamics of the water molecules for the interfacial and core regions to find that the slower dynamics persists even for the core water for the size range that we have studied although to a much lesser extent as compared to the interfacial water. Moreover, we demonstrate that the hydrophobic interface in the water-in-oil nanodroplets has much weaker effect on the structure and dynamics of the confined water molecules as compared to the anionic RMs. Thus, the major contribution towards the structural ordering and slow dynamics of water in a charged RM system would

originate from the strong electrostatic and hydrogen bonded interactions with the interface, and not due to the spatial confinement effect.

Introduction

Despite being a deceptively small molecule water remains an enigma to the scientific community.[1, 2] Not only does it have a wide array of anomalous bulk properties,[3] "water under confinement" and "interfacial water" have turned into active areas of research due to the staggering diversity of context dependent properties of water.[4-14] Most of the functional roles of water in both biological and materials science context originate due to the unique properties of interfacial and/or confined water, e.g. cellular water exists in a highly crowded and confined medium, surface water molecules dictate the phenomena like hydrophobic collapse and self-assembly, and water may experience extreme confinement in clays, minerals as well as deep interiors of functional sites in biomolecules.

Reverse micelles (RM) and water-in-oil microemulsions (W/O) have been popular choices as model systems to study physicochemical properties of water under confinement and crowded environment, as well as various chemical and biomolecular processes under confinement, e.g. protein folding, enzyme catalysis, light induced charge separation, proton transfer and so on.[4, 5, 12, 15-20] Sodium bis(2-ethylhexyl) sulfosuccinate (AOT) is one of the most commonly used surfactant with anionic head groups to study reverse micelles.[4, 8, 21-23] In the last few decades, the shape, size and composition of RMs as well as the structural and dynamical properties of the water molecules confined in these RMs have been studied extensively using a wide range of experimental techniques like NMR, small angle X-ray scattering (SAXS), dynamic light scattering (DLS), quasielastic neutron scattering (QENS), vibrational spectroscopy and

spectral diffusion, dielectric relaxation, solvation dynamics studies and so on.[4, 7, 9, 16, 18, 22, 24-32] The experimental studies have often been motivated and complemented by an impressive amount of theoretical and computational studies that have built the foundation of our current understanding of the unique properties of water under confinement and interfacial water.[6, 8, 11, 12, 19, 20, 33-40]

Through the extensive body of research developed over last few decades it has been well established that the water under confinement may exhibit drastically different physicochemical properties as compared to bulk water. Confined water may have reduced polarity (dielectric constant), a perturbed hydrogen bonded network, and structural ordering at the interfacial region among many others.[35, 40-42] Dynamical properties of water are highly affected by the confinement as well, e.g. both orientational dynamics and translation mobility along with dielectric relaxation of water slows down considerably for interfacial water.[19, 21, 27, 32, 36, 38, 43-45]

Spatial confinement is only one of the factors that might affect the water properties in RMs. Since the interior surface in RMs is most commonly charged or polar depending on the surfactant composition, the water molecules can have a strong binding affinity to the interior surface. Thus, the slower exchange between the "bound" interfacial water and "free" core water leads to the observed slow dynamics near the surface region.[12, 19] A core-shell type of model has often been invoked where the shell consisting of the interfacial water would have drastically different properties than bulk water, and the water molecules further away from the interface (core water) would gradually recover the bulk-like characteristics as the distance from the interface increases for larger RMs. This hypothesis has been examined both experimentally and by simulation studies by varying the size of the RMs, since it can be expected that if the size of the water pool gets bigger, the relative ratio of "bulk-like" core water molecules should

increase.[26, 27] The effective size of RMs and hence the size of the confined water pool is usually controlled by the water loading ratio given by $w_0 = [H_2O]/[AOT]$. Multiple studies have suggested that the water dynamics in the core region of the RMs for larger RMs ($w_0 > 10$) gradually recovers the bulk-like characteristics.[21, 26, 27, 36, 38, 46].

Using theoretical vibrational spectroscopy and simulation studies, Skinner and coworkers have nicely demonstrated that the distance dependence of the water dynamics from the interface as well as the length scale over which the bulk properties would be recovered, are dependent on the RM size due to the curvature induced effects, which is in clear contradiction with a simple core-shell type model of water dynamics in RMs.[6] They have also shown that the rotational anisotropy dynamics reaches bulk-like characteristics beyond 0.8nm distance from the interface for w_0=7.5. On the other hand, it has been speculated in different contexts that water mediated interactions induced by dipolar correlations between large polar (and even non-polar) interfaces might extend across several nanometers.[47, 48] Thus, one may not rule out that the length-scale over which water properties may vary as a function of distance from the interface, might depend on the water property that is being probed, namely local spatial order, translational order versus global dipolar orientation/correlation. Bagchi and coworkers have put forward a somewhat similar argument in the context of water interface with hydrophobic surfaces.[49] They have suggested that the spatial (translational) structural ordering may not be as long range as the orientational (or tetrahedral) structural ordering of water, where the orientational order may sustain longer range correlations. Thus, the length-scale of water structure being perturbed by an external interface may depend on whether we are investigating the translational order versus orientational order.

Fayer and coworkers have also suggested that a simple distinction between interfacial and bulk-like core water may not be possible depending on the water property that is being investigated.[26] In particular, they find that the size dependence of the hydroxyl stretch absorption spectra and vibrational population relaxation times can be well described by an appropriately weighted average between the bulk water and small RMs (w_0=2; all water molecules are assumed to be interfacial), whereas the same model does not perform well for spectral diffusion and orientational relexation due to long range coupling between the interfacial and core regions. Thus, depending on the sensitivity of the property/phenomena of interest on the perturbations induced by the environment, we may observe different behavior.

In an attempt to dissect to relative role of spatial confinement versus the specific interactions with the RM interior surface, several studies have compared the water dynamics inside charged and neutral RM systems.[31, 50, 51] Surprisingly, water dynamics near both charged and neutral hydrophilic interfaces has been found to be comparable and slower compared to bulk water. Thus, it has been concluded from these studies that the overall hydrophilic nature of the interface and the spatial confinement effects lead to the slow dynamics of interfacial water, whereas the specific chemical composition of the interface plays only a secondary role. On the other hand, the simulation studies by Laage and Thompson on the water dynamics in hydrophilic and hydrophobic nanoporous medium clearly demonstrate that slowing down of water dynamics is only modest in the case of hydrophobic cavities.[52] Thus, the spatial confinement effects may not contribute to the slower orientational dynamics observed in hydrophilic confinement (either neutral or charged), which should originate due to the favorable hydrogen bonding interactions between the surface and interfacial water molecules.

The above discussion clearly highlights the need of a systematic investigation of the various types of structural and dynamical properties of water in both hydrophilic and hydrophobic confinement as a function of the size of the confinement as well as the distance dependence of the properties from the interface as they approach bulk-like characteristics. In this work, we investigate three different types of structural order parameters, namely (i) local density (spatial order), (ii) local tetrahedral order and hydrogen bond distribution (local orientational order) and (iii) average dipolar orientation (global orientational order). We have also investigated the orientational and translational (diffusion) dynamics of the water molecules in a layer-wise fashion. The effect of confinement size has been studied using three different sizes of AOT RMs (w_0=10, 15 and 20), which are relatively larger in size as compared to prior MD simulation studies enabling us to actually observe the bulk-like characteristics instead of using extrapolation techniques. Our results clearly demonstrate that whether the water present inside a RM is bulk-like or not and the effective size of the bulk-like core water region would strongly depend on the choice of order parameter (i.e. translational versus orientational).

Moreover, in order to clearly distinguish between the effects of "confinement" versus the proximity to a "hydrophilic" surface on the water properties, we have systematically compared the behavior of water in RMs with the control systems of water-in-oil (isooctane) nanodroplets with the identical number of water molecules as the respective RM systems. The water-in-oil (W/O) systems would allow us to separately understand the effect of confinement on the water in the absence of the AOT surfactants (negatively charged interface). Of course, the structure and dynamics of water molecules in the water-oil interface have been actively studied through decades.[13, 14, 53-60] In the limited scope of our work, we present a systematic size dependent

comparison of the water structure and dynamics in both the RM and W/O systems to highlight the key factors that lead to the unique behavior of water inside RMs.

The rest of the paper is organized as follows: we first give details about our computational methodology. In subsequent sections we analyze (i) the radial profiles of various structural order parameters, (ii) the region-wise (interfacial and core) probability distributions of these order parameters to demonstrate that the deviations from bulk-like characteristics is strongly dependent on the property of interest, and (iii) the orientational and translational dynamics in both RM and W/O systems. Finally, we provide our concluding remarks.

Computational details

We have used three different sizes of the reverse micelle (RM) systems corresponding to the molar ratio $[H2O]/[AOT] = w_0 = 10, 15$ and 20 in the increasing order of size. Corresponding three water-in-oil nanodroplet systems (W/O) have been prepared by keeping the number of water same as the $w_0 = 10, 15$ and 20 RM systems, where the water pools have been surrounded by the isooctane molecules. For the AOT RM systems we have added same number of Na^+ counter-ions as AOT molecules in order to charge neutralize the whole system and the ions have been added at close proximity to the AOT head groups as clarified in Table S1 (in SI). The numbers of water, AOT, Na^+ ions and isooctane molecules used for preparing the above six systems are shown in Table 1. During the subsequent discussions, we shall refer to the RM systems by $w_0 = 10, 15$ and 20, whereas the water-in-oil systems will be referred as W/O = 10, 15 and 20, respectively. The number of AOT and water molecules, and the packing radii for the different water loading of RM systems have been taken from existing NMR data,[24] which has been subsequently used in other simulation studies as well.[15, 61] These structural parameters are

in agreement with the aggregation number and radii derived using other experimental techniques as well.[26, 46, 62, 63] The initial structures for the RM and W/O systems have been created using the Packmol software, where each molecular species has been packed within a certain spherical cut-off radius as used by Abel et al.[15] The chosen packing radii for the inner water pool, counter-ions and the outer sphere of AOT monolayer have been provided in Table S1 (in SI) for every system studied here.

The AOT surfactant and isooctane molecules have been modeled using the CHARMM27 all-atom force-field following the protocol used by Abel et al.[15] Although TIP3P water model is commonly used with CHARMM force field, we have shown earlier that this water model does not capture the tetrahedral ordering of water molecules correctly.[64] Thus we have used the more recent TIP4P/2005 water model, which has been shown to perform quite well in reproducing a wide range of bulk water properties.[65, 66] Since our primary goal is to investigate the structural and dynamical properties of water, we feel that choice of a better water model is very important.

We have used the GROMACS (version 5.0.7) software suite[67] for the molecular dynamics simulations reported here. Periodic boundary conditions have been applied in all directions. In every case the simulation box dimension has been chosen such that the distance between surface of the AOT RM or the water pool in W/O system and the box boundary is at least 1nm to avoid any short range interaction between the periodic images. All bonds have been constrained to their equilibrium bond lengths. We have used a cutoff of 1.0nm for both short-range coulomb and Van der Waals interactions. The long-range electrostatic interactions have been treated with particle mesh Ewald method with 0.16nm of grid spacing. Before starting the molecular dynamics simulations, we have performed energy minimization using steepest-descent algorithm in order to remove any clashes between the molecules. Afterwards NVT equilibration

has been performed for 2ns at 300K temperature using the V-rescale thermostat[68] and NPT equilibration has been performed at 1 bar pressure and 300K temperature using the Berendsen barostat[69] for the duration of 2ns for W/O systems and 20ns for RM systems. We have used the Parinello-Rahman barostat[70] during the production runs, with 2fs integration time step and the trajectory frames have been saved every 1ps for subsequent analysis. The total production run lengths for various systems have been provided in Table 1. Additionally, we have performed simulations for bulk water as the reference system for comparison with various confined water systems. In this case, the NVT and NPT equilibration run lengths have been 1ns each with all other details remaining the same as described above.

RESULTS AND DISCUSSION

Nature of the confinement: Reverse micelle vs. water-in-oil nanodroplet

The structure and dynamics of water under confinement have been well studied using a wide variety of surfactant molecules including cationic/anionic/neutral.[31, 50, 51, 71] All of these systems are characterized by a hydrophilic interior surface, where water can preferentially bind. Although the strength of the interaction between interfacial water and the RM interior wall may depend on the charge distribution of the surface, it is expected that the favorable interactions would lead to a slower exchange between the interfacial and core water molecules leading to the traditionally observed slower dynamics in these systems. Thus, in addition to the confinement effect (size of the water pool), the reverse micelles also provide an additional perturbation of a strongly hydrophilic interface due to the favorable electrostatic interaction with the interface.

In order to dissect the relative role of size induced "confinement" versus the charged surface induced "binding/ordering" at the interface, we have taken up the reference systems of

water-in-oil nanodroplets, where we keep identical number of water molecules (as compared to the RM systems of $w_0 = 10$, 15 and 20) in a hydrophobic isooctane background. In the absence of any AOT surfactant molecules, these systems would allow us to investigate the purely confinement size induced perturbations in the water nanodroplets in the absence of any hydrophilic interfaces.

Our molecular dynamics trajectories show quite stable quasi-spherical water pools in both RM (3 sizes) and W/O (3 sizes) systems. Representative snapshots from the MD trajectory have been shown in the Fig. 1 for the $w_0 = 10$, 15, 20 and W/O = 20 systems. On the left panels we include the surrounding isooctane medium, whereas the right panel zooms into the RM and W/O interior. The AOT head groups and counter-ions have been clearly identified as visual guideline to the interfacial regions.

We have observed considerable shape fluctuations (deviations from spherical shape) in the AOT RM systems. Similar observations have been made before using both dynamic light scattering experiments and MD simulations of RMs by Straub and coworkers.[8, 22, 72] The shape fluctuations seem to be particularly pronounced in smaller RMs.[22] We have shown the time evolution of the radius of gyration (indicator of size) and the anisotropy shape parameter (ratio of smallest and largest principal components of the gyration tensor, which would be 1 for perfect sphere) in the Fig. S1 (in SI). The time evolution of radius of gyration shows that both the RM and W/O systems maintain a relatively compact structure with considerably higher fluctuations for the RM system. But the RM structures remain stable and intact throughout the 100ns trajectory for each system. Whereas, the shape anisotropy parameter indicates that the deviations from spherical symmetry is remarkably higher in the RM systems as reported earlier by Straub

and coworkers,[8] whereas the W/O systems seem to retain much higher degree of spherical nature.

In the subsequent sections we shall demonstrate that both the structural and dynamical properties of water between these two systems are drastically different. Despite being a confined system, the water molecules in a W/O nanodroplet show remarkable similarity to bulk water even for the smallest size (W/O=10) for most of the properties studied in this work. The deviations from bulk-like properties are not significant as compared to the RM systems even for the interfacial water (except for a few properties) in these systems as will be demonstrated below.

Choice of the structural order parameters

We have used three classes of structural order parameters in order to probe both the translational and orientational ordering of the water molecules under confinement of RM and W/O systems. The chosen order parameters are:

(i) **Number density (ρ):** The number of water molecules present per unit volume for different probe regions. This quantity would capture the local translational ordering (density) of the water molecules as compared to the bulk water density.

(ii) **Tetrahedral order parameter (Q) and number of hydrogen bonds (N_{HB}):** Following the prescription of Debenedetti and coworkers,[3] we have used the following definition of tetrahedral order parameter of water:

$$Q_i = 1 - \frac{3}{8}\sum_{j=1}^{3}\sum_{k=j+1}^{4}\left(\cos\theta_{jik} + \frac{1}{3}\right)^2 , \qquad (1)$$

where, Q_i is the tetrahedral order parameter of the i-th water molecule and θ_{jik} is the angle

subtended on the oxygen atom of that water molecule by the each pair (given by the indices j and

k) of four nearest neighbor molecules. Thus, for a perfectly tetrahedral arrangement of the four

neighboring water molecules around the central i-th water molecule $Q=1$, whereas for a random

and uniform distribution of these angles $Q=0$.

　We have used the following geometric criterion for detecting the hydrogen bonds between

water molecules: (i) the O-O distance between the donor and acceptor molecules is less than

0.35nm, and (ii) the H-O (donor)-O (acceptor) angle is less than 30 degrees. For both the

tetrahedral order parameter and hydrogen bond calculations we have included the O atoms of the

AOT head groups among the possible neighbors (for Q) and hydrogen bond acceptors (for N_{HB})

for the water molecules, since the interfacial water molecules preferentially forms hydrogen

bond with the AOT head groups at the expense of losing water-water hydrogen bonds.[33]

　Interestingly, for all subsequent analyses we find that the variation in the average and

probability distribution of tetrahedral order parameter follows an identical trend as the number of

hydrogen bonds, since both of these quantities capture the local tetrahedral order and hydrogen

bonding pattern of the water molecules. Thus, we report only the data for tetrahedral order

parameter here, since it shows slightly higher sensitivity to environmental changes due to the

inherent discrete nature of the number of hydrogen bonds.

　(iii) Dipolar orientation relative to the radial vector (P): Being an isotropic medium there is

no net dipolar orientation in bulk water, whereas near a charged interface the water dipoles are

likely to have a preferred direction of orientation. We have quantified the dipolar orientation (P)

as:

$$P = \frac{\vec{r} \cdot \vec{\mu}}{|\vec{r}| \cdot |\vec{\mu}|} = \cos\theta \quad , \tag{2}$$

where, $\vec{r}$ is the radial vector from the oxygen atom of a water molecule to the center of mass (COM) of the water pool, $\vec{\mu}$ is the dipole moment vector of that water molecule. The angle between these vectors (θ) would be zero if the water dipole is pointed towards the COM. We have used the cosine of the angle ($\cos\theta$) for describing the orientational polarization of the water molecules.

Radial profiles of the structural order parameters

It has been well established that the interfacial water in reverse micelles have distinctive structural and dynamical properties as compared to bulk water. Thus, we expect that the water molecules further away from the interfacial region should gradually recover their bulk-like characteristics. In other words, the central core region of the confined water pool is likely to have closer resemblance to the bulk water. Moreover, the effective size of this bulk-like core water region is expected to increase with the overall size of the water pool.

In order to investigate the above hypotheses, we have first calculated the radial profiles of the three structural order parameters described above for both the RM and W/O systems for all three sizes. The comparison between these radial profiles has been shown in Figs. 2(a-c). Here we have constructed spherical shells (with increasing radius in the range of 0.3 nm to 5 nm) around the center of mass (COM) of the water pool with the thickness of each shell being 0.1 nm. All the radial profiles have been obtained by averaging the corresponding properties for all water molecules lying within the radial shells. Thus, the radial profiles describe the average

structural order parameters as function of distance from the COM of the water pool towards the interfacial region. We expect the bulk-like behavior at smaller radius (nearer to the COM) and the departure from the corresponding bulk property (shown in black line in each case) would signify the boundary of a spherical bulk-like core region.

Fig. 2a summarizes the radial number density profiles in both RM (3 sizes) and W/O (3 sizes) systems. We observe that all the systems demonstrate a flat region (constant value) near the COM signifying a core region where the water density is uniform and almost identical to the bulk water value (33.2 nm^{-3}). The number density slightly increases for smaller systems, since the higher curvature of the interfaces in smaller confined systems would induce a higher internal pressure on the internal water. Interestingly, the W/O systems demonstrate a much sharper drop in the density profile as compared to the RM systems, since they retain higher degree of spherical nature as compared to the RM systems. Thus, the drop in the number density coincides with a well-defined radius of the water pool. In contrast, the RM systems undergo substantial shape fluctuations and a radial average over these fluctuations give rise to a slower fall in the density profile. Nevertheless, the radii of the core regions with bulk-like water density for the RM systems are approximately 1nm, 1.8nm and 2.5nm for w_0=10, 15 and 20, respectively. For W/O systems these regions are larger by ~0.7nm in each case. The effective radii of each studied system can be directly deduced from the interfacial sharp drop in the radial profile. The effective radii of water pool for the RM and W/O systems are consistent to the prior small angle X-ray scattering measurements[25] and viscosity measurements.[73]

The radial profiles of the tetrahedral order parameter have been compared in Fig.2b. The profiles follow similar qualitative trends as the number density profiles, i.e. there is a core region with bulk-like value and the tetrahedral order gradually decreases to zero across the interfacial

region. Interestingly, we notice that the radii of the spherical regions with bulk-like value (~0.67

for TIP4P/2005 water model) have become smaller by ~0.3nm as compared to the corresponding

density profiles. Thus, the tetrahedrality or orientational order of the water molecules is

perturbed to a slightly larger lengthscale by the interface as compared to the number density.

Moreover, the difference between the RM and W/O systems has become more pronounced in the

tetrahedral ordering. While for the W/O systems the radial profile drops almost as sharply as the

number density profiles, it changes much more slowly for the RM systems. This evidently points

towards the fact that the negatively charged interface in the AOT RM system affects the

tetrahedral order of the water molecules due to the long range electrostatic interactions, which

can be either direct perturbation or gradually propagated through the structural changes of

intermediate water molecules.

Finally, we compare the dipolar orientation of the water molecules with respect to the

radial vector in Fig. 2c. Remarkably, the radial profiles of $\left\langle \cos\theta \right\rangle = \left\langle \dfrac{\vec{r} \cdot \vec{\mu}}{\left|\vec{r}\right| \cdot \left|\vec{\mu}\right|} \right\rangle$ for the RM and

W/O systems show a huge difference. In bulk water, the dipole vectors of the water molecules

should not have any preferential orientation since the medium is fully isotropic. Thus, the

reference calculation performed in bulk water (black line) shows a constant value of zero.

Similarly, for all the W/O systems the core water region is devoid of any orientational

preference. Only near the interface of these systems we observe an oscillatory behavior around

zero due to certain orientational constraint imposed on the water molecules at the interface. But

for all of the RM systems the radial profile remains non-zero ($\left\langle \cos\theta \right\rangle > 0$) for almost whole

water pool. Even for the largest RM system (w_0=20), the approach towards $\left\langle \cos\theta \right\rangle \to 0$ is very

slow as we approach from the interfacial region to the deeper core of the water pool. The

predominantly positive values of $\langle \cos\theta \rangle$ at all radial shells would signify that the electrostatic field due the negatively charged interior surface would orient the dipole vector of the water molecules away from it, thus creating a substantial preferential orientation of the water molecules towards the COM of the water pool.

The overall physical picture obtained from the above analyses has been schematically described in the Fig.3. Here we have identified two regions in the water pool based on the distance from the interface, namely "interfacial water" (<1.1 nm from the S atoms of the AOT head groups) and "core water". The concentric circles in the "core water" region clearly delineate the zones resembling the bulk-like characteristics based on the water property that is being investigated. While the number density becomes bulk-like much closer to the interface, the tetrahedral ordering of water (and hydrogen bonding pattern) is affected to longer distance. The dipolar orientation is affected the most in a RM system (> 3nm from the interface).

Distribution of the structural order parameters: Core versus interface

The radial profiles shown in Fig. 2 clearly distinguishes the bulk-like behavior (or lack thereof) of the core water region using various structural order parameters. But, due to the substantial shape fluctuations (deviations from spherical shape), the spherical symmetry is lost, particularly in the RM systems.[8, 22] Thus, the radial profiles are not sufficient to study the characteristics of the interfacial regions, since the spherical shells might be averaging over both the interfacial and core water molecules depending on the radius of the shell and shape of the RM. The schematic picture shown in Fig. 3 clarifies this issue due to spherical asymmetry. The deviations from spherical structure in the RM systems have been highlighted through the shape anisotropy parameter, which is the ratio of smallest to largest component of the gyration tensor, as shown in

the Figure S1(b). The anisotropy parameter values for the W/O systems remain above 0.9, whereas for the RM systems it undergoes huge fluctuations in the broad range of 0.6-0.9.

In order to clearly delineate between core and interfacial water molecules, we have used a different protocol of dividing the water molecules based on the distance from the interface. Based on the radial distribution function of water from the interface (data not shown) and earlier simulation studies where a distance cut-off ≤ 1 nm had been used,[33] we have decided to use a comfortable margin of 1.1 nm to define the "interfacial water" so that the "core water" remains far away from the interface. Subsequently, we compute the probability distributions of the structural order parameters separately for the "core water" and "interfacial water" molecules in order to investigate their possible deviations from bulk properties.

We have outlined the distribution of number density (ρ) separately for core and interfacial water in Figs. 4a and 4b, respectively. The core water in the RM systems shows almost identical density distribution as bulk water. However, the smaller W/O systems (W/O = 10 and 15) demonstrate lowering of population at bulk-water density and develops a tail distribution at lower density. In the interfacial region, this variation is even more pronounced (Fig. 4b). We must clarify here that a sub-population of the interfacial water molecules exactly at the boundary of the interface would not have enough number of nearest neighbors to satisfy the bulk-like number density, thus the local average coordination number (density) is expected to be lower than bulk value for interfacial water. So we expect a tail distribution at lower density values as compared to bulk water both for interfacial water in RM and W/O systems. Interestingly, we observe that while the density distribution in the RM systems show the peak at the same position as bulk water, for the W/O systems it drastically shifts to much lower values. Of course, there exists a shoulder-like tail at lower densities for the RM systems as expected. The

lowering of surface density near an extended hydrophobic surface has been well documented

before and it has been suggested that the local water density undergoes large scale density

fluctuations near extended hydrophobic surfaces.[58, 59, 64] We feel that similar factors are leading

to the large deviations in the local density distribution for the interfacial water in W/O systems.

In contrast, the hydrophilic anionic interface in the RM systems reinstates the water density

leading to a discernable population of water molecules with bulk-like coordination number.

Figs. 4c and 4d show the similar distributions for the tetrahedral order parameter. The

tetrahedrality displays bulk-like characteristics (with very minor decrease) across the systems for

the core water molecules. On the other hand, for the interfacial water there is a distinct decrease

in the tetrahedral ordering. Interestingly, the W/O systems demonstrate lower tetrahedral order

than the RM systems in the interfacial region. While the hydrophobic interface in the W/O

systems induces large perturbation on the hydrogen bonded network of the interfacial water, the

negatively charged interface reinforce this due to preferential hydrogen bonding between water

and the AOT head groups. While the interfacial water molecules may lose certain amount of

water-water hydrogen bonds, this is counterbalanced by the preferential hydrogen bonding

between the AOT head groups and the interfacial water molecules.[33] Thus, the overall tetrahedral

order or hydrogen bonding pattern is preserved to some extent in the RM systems. We have also

compared the hydrogen bond distributions between these regions, but the data has not been

shown here since the trends are almost identical to the tetrahedral order parameter distributions.

The distributions of the dipolar orientation ($\cos\theta$) in the core and interfacial region have

been shown in Figs. 4e and 4f. As discussed in the radial profiles of the same property (Fig. 2),

in an isotropic bulk liquid all possible orientations are equally likely. Thus, $P(\cos\theta)$ remains

constant for bulk water. The same scenario holds for the core water in the W/O systems, where

there is no long range electrostatic perturbations from the interface. Of course the interfacial water shows a non-uniform distribution even for the W/O due to the preferential orientation of the water dipoles to remain parallel to the interface. On the other hand, for the RM systems not only the interfacial water, but even the core region demonstrates a preference towards an orientation towards the COM of the water pool as discussed earlier in the context of the radial profiles.

Orientational relaxation dynamics: Core versus interface

The dynamics of the water molecules in the reverse micelles has been studied extensively in the past.[8, 9, 26, 37, 52, 74, 75] But how do the orientational and translational dynamics compare between the RM and W/O systems? We have addressed this question by studying the orientational relaxation of the water molecules separately in the core and interfacial regions, by using the following orientational time autocorrelation function (OTCF):

$$C_\mu(t) = \frac{\langle \vec{\mu}_i(t) \cdot \vec{\mu}_i(0) \rangle}{\langle \vec{\mu}_i(0) \cdot \vec{\mu}_i(0) \rangle} , \tag{3}$$

where, $\vec{\mu}_i(t)$ is the dipole vector of the ith water molecule at time t. The averaging is performed over the water molecule which stays continuously in the selected region for the time interval of 0 to t in order to avoid the mixing of dynamics when a water molecule is exchanged between the interfacial and core regions. Depending on the size of the RM system and associated heterogeneity in the time scales present in the system, the OTCF can be fit well by either single exponential or multi-exponential or stretched exponential or power law functions as reported in earlier studies.[8, 26, 52] In our work, we have used a tri-exponential fit of the OTCF to compare the

time scales observed across all of the seven systems (including bulk water). The time scales and their relative contributions have been reported in Table 2 for core and interfacial regions across all the systems. For the shorter survival time of ~50ps of water molecules in the respective region, OTCFs fits well to the tri-exponential fitting function. For the long-lived tails of correlation functions, both fitting functions fail to catch the decay times as reported earlier.[8]

Figs. 5a and 5b show the comparison of OTCF across all systems for the core and interfacial water, respectively. A visual inspection of the figures clearly shows that for the W/O systems the orientational dynamics is almost identical to the bulk water, while the time scales are slightly higher for the interfacial water. In contrast, for the RM systems the interfacial water undergoes a dramatic slowdown (more than an order of magnitude) as demonstrated through a multitude of prior experimental and simulation studies. We observe that the slowest component of the OTCF in the interfacial region of RMs fall in the range of ~100ps (Table 2), which is in very good agreement with prior simulation studies.[39] Interestingly, the increase in the slowest time component in the interfacial water of the W/O systems is very small (~10ps) as compared to bulk water (~6ps). This clearly confirms the role of the hydrophilic interface in the RM systems towards the observed slow dynamics. Since the free energy of binding of water to the RM surface is much stronger compared to the W/O systems, the exchange rate of the bound water molecules is likely to be much smaller as well.

Interestingly, even for the core water in the RM systems a slight slowdown is visible. The comparison of the time scales observed for the core water (Table 2) clearly shows that for RM systems the slowdown remains to certain extent even beyond 1.1 nm distance from the interface. The time scales are ~45ps, ~27ps and ~24ps for w_0 = 10, 15 and 20, respectively. This long range slowdown is likely to originate from the long range electrostatic interactions with the

charged interface, since such slowdown is completely absent in the core water for W/O systems. Moreover, the dependence of the water dynamics on the distance from the interface might be slower compared to our chosen distance cut-off of 1.1nm to distinguish between the interfacial and core water. Thus, a core-shell model with clear demarcation between "interfacial" and "core" water might be too simplistic as indicated by prior experimental studies[9, 26, 27]. For example, according to the simulation studies by Skinner and coworkers[9] the rotational anisotropy reaches bulk value at a distance of 0.8nm from the interface for w_0=7.5, whereas this distance dependence is much slower for smaller RMs due to curvature induced effects. On the other hand, simulation studies of water dynamics around micelles[36] indicate that interfacial effects may sustain upto 2nm distance from the charged interface of the micelle. Our observations regarding the long range perturbations on the global dipolar orientations that might extend upto 3nm from the RM interface also suggests the possibility that certain water properties might be more sensitive with longer length-scale of perturbation. Thus, a more detailed layer-wise decomposition of various types of water dynamics (vibrational, rotational, collective modes, dielectric relaxation etc.) as a function of distance from the interface would be necessary to shed light on the length scale of such interfacial perturbations.[37, 74] Although we can safely conclude that bulk-like dynamics can be observed in reverse micelles with water pool diameter larger than 4nm (w_0>20) as confirmed by Fayer and coworkers.[26, 27]

Previous experimental studies have shown that the hydrogen bond orientational relaxation timescale is almost similar for the neutral and ionic interfaces concluding that the hydrophilic interface and confinement play a dominant role, while the specific chemical nature of the interface plays a secondary role.[31, 50, 51] We argue that the comparison between neutral and charged RM systems does not separately investigate the effect due to the purely spatial

confinement in a clean way, since both systems have hydrophilic interfaces that strongly interact with the water molecules leading to the observed slow dynamics. In the present study, we have dissected the effect of confinement versus the presence of a hydrophilic interface to conclude that the spatial confinement does not affect the orientational dynamics of the interfacial water molecules. Our results are in good agreement with the work of Laage and Thompson [52] showing that the OH reorientation in water is significantly slower in hydrophilic confinement compared to the bulk water, whereas the dynamics of water in the hydrophobic pores are more modestly affected.

Diffusion of water: Core versus interface

Next we compare the translational mobility of the core and interfacial water in the RM and W/O systems by monitoring the respective mean square displacement (MSD) versus time, i.e. $\left\langle \Delta r^2 \right\rangle(t)$ (Figs. 6(a-b)). Since the water molecules are likely to be exchanged between the core and interfacial regions, we have restricted the averaging of MSD for those fragments of the trajectory where a water molecule stays continuously for the chosen time interval of 0 to t ps. Here we have focused on the short time dynamics (< 200ps), since the MSD reaches a plateau beyond a certain time scale due to the spatial confinement. There is a characteristic timescale for each system beyond which the water molecules reach the limits of the confinement size and hence MSD cannot grow any further. Moreover, for this reason we do not include the data for the smallest water pool systems (w_0=10 and W/O=10) for MSD analysis, since we have been unable to generate statistically significant data due to relatively small residence time in the interfacial/core regions in these cases.

As we compare the MSD curves of all the systems, we find that the core water molecules in W/O systems are consistently faster than the RMs (Fig. 6a), and they are much closer to the bulk-like behavior. The translational mobility monotonically increases with the size of the water pool in each system. Interestingly, for the W/O systems there exists a short-to-intermediate time scale (<50ps) where the MSD goes slightly above the bulk MSD (possibly due to the absence of long range electrostatic interactions and lower polarity of the W/O water pool as compared to bulk), but subsequently they start to grow much slower than the bulk water as expected. The difference in mobility between RM and W/O systems become particularly pronounced for the interfacial water, where the water in RM systems show ~4 times slower diffusion as compared to the W/O systems. For the interfacial water, we find much weaker size dependence in the RM systems. This indicates towards the fact that there exists a characteristics timescale of "interfacial water" that can be independent of the size of the "core water" pool. The slower translational dynamics of the interfacial water molecules have the same molecular origin as the corresponding orientational dynamics. The strong electrostatic and hydrogen bonding interactions between the interfacial water and the charged AOT head groups would considerably increase both the residence time and the hydrogen bond lifetime in this region.[72] However, in W/O systems, such strong perturbation is absent leading to bulk-like diffusivity even for the interfacial water.

Finally, we characterize whether the translational motion of the water molecules are diffusive or sub-diffusive in nature. For this purpose, we evaluate the linearity of the time dependence of MSD, i.e. for $\langle \Delta r^2 \rangle(t) \propto t^{\beta}$, where $\beta = 1$ and $\beta < 1$ would signify diffusive and sub-diffusive motions, respectively.[37] We compute the exponent β as the slope of the log-log plot of MSD as shown in Figs. 6c and 6d for core and interfacial water, respectively. Our results clearly indicate that water under confinement remains sub-diffusive (β < 1) consistently across

all systems and sizes. Of course, the time scale at which the bulk water attains the perfect diffusive regime ($\beta = 1$) is slightly larger than the time scale at which we have managed to gather sufficient statistics for confined water due to the limitations of residence time. Nevertheless, we can qualitatively conclude that the W/O systems display a higher degree of similarity to the bulk water as compared to the RM systems. As usual, for the interfacial water this difference is remarkably pronounced and sub-diffusive dynamics persists for both RM and W/O systems.

Conclusion

We have presented a systematic investigation of three different kinds of structural order parameters, and translational and rotational dynamics of water molecules in the confinement of AOT RMs and W/O nanodroplets as a function of their sizes in the quest of characterizing the deviations from bulk-like behavior in these confined systems. We demonstrate that the characterization of confined water as "bulk-like" water would strongly depend on which property of water we are looking at. While the translational order parameters tend to be less perturbed by the interface, the tetrahedral and orientational order parameters have long range perturbations due to the presence of charged/hydrophilic interface in the AOT RMs. Moreover, we show that the global orientational ordering of the water molecules may persist to a much larger length-scale (~3nm) from the charged interface, as compared to the local orientational ordering due to hydrogen bonded network. Interestingly, previous simulation studies in reverse micelles have shown that the rotational anisotropy time-scale may reach bulk behavior beyond a distance of 0.8nm from the interface for w_0=7.5.[6] This wide mismatch between the length-scales leads to a very significant conclusion that the local orientational dynamics might be dictated by the local environment and local hydrogen bonded network of the probe water molecules, whereas the

overall global dipolar orientational ordering may sustain to much longer length-scales near charged interfaces. This observation might have significant implications towards earlier suggestions that long range dipolar correlations might lead to attractive interaction between polar (and even non-polar) interfaces over a length-scale of several nanometers.[48]

We have further dissected the relative effect of the size induced confinement versus the perturbation due to the charged interface by comparing all properties with respect to the model control systems of W/O nanodroplets with same size as corresponding RM systems. We clearly demonstrate that the effect of confinement in the W/O systems is almost negligible as compared to the pronounced effect on the water structure and dynamics in the RM systems. Previously, the observation of similar interfacial water dynamics in neutral and charged RM systems have led to the conclusion that either the spatial confinement or hydrophilic interface causes the slowdown, and the specific chemical nature of the interface has only a secondary role. We argue that while the local orientational order and dynamics might remain similar between the neutral and charged interfaces due to the hydrophilic nature of the interfaces, (i) the long range orientational order would be substantially different between the systems, and (ii) in the absence of a hydrophilic interface the slowdown becomes negligible, thus ruling out the possible role of spatial confinement effects. Thus, our results clearly delineate the major role of long range electrostatic interactions and the high binding affinity of the water molecules to the hydrophilic RM interior surface in contrast to the spatial confinement effects.

Interestingly, we find that the dynamical properties of water have higher degree of sensitivity to the environmental perturbations as compared to the structural order parameters. The translational dynamics shows substantial sub-diffusive behavior in both RM and W/O systems. Thus, this is the only water property where both RM and W/O systems show significant

departure from bulk behavior. Thus, we may also conclude that the translational dynamics can be significantly affected by the pure spatial confinement effect, whereas all other structural order parameters and orientational dynamics are only perturbed by the electrostatic interactions in the RM systems.

Acknowledgements

References

1.   B. Bagchi, *Water in Biological and Chemical Processes: From Structure and Dynamics to Function*, Cambridge University Press, 2013.
2.   P. Ball, *Chemical Reviews*, 2008, **108**, 74-108.
3.   J. R. Errington and P. G. Debenedetti, *Nature*, 2001, **409**, 318-321.
4.   N. E. Levinger and L. A. Swafford, *Annual Review of Physical Chemistry*, 2009, **60**, 385-406.
5.   M. D. Fayer and N. E. Levinger, *Annual Review of Analytical Chemistry*, 2010, **3**, 89-107.
6.   P. A. Pieniazek, Y.-S. Lin, J. Chowdhary, B. M. Ladanyi and J. L. Skinner, *The Journal of Physical Chemistry B*, 2009, **113**, 15017-15028.
7.   M. R. Harpham, B. M. Ladanyi, N. E. Levinger and K. W. Herwig, *The Journal of Chemical Physics*, 2004, **121**, 7855-7868.
8.   A. V. Martinez, L. Dominguez, E. Małolepsza, A. Moser, Z. Ziegler and J. E. Straub, *The Journal of Physical Chemistry B*, 2013, **117**, 7345-7351.
9.   J. L. Skinner, P. A. Pieniazek and S. M. Gruenbaum, *Accounts of Chemical Research*, 2012, **45**, 93-100.
10.   N. E. Levinger, *Science*, 2002, **298**, 1722-1723.
11.   B. Bagchi, *Chemical Reviews*, 2005, **105**, 3197-3219.
12.   N. Nandi, K. Bhattacharyya and B. Bagchi, *Chemical Reviews*, 2000, **100**, 2013-2046.
13.   S. Romero-Vargas Castrillón, N. Giovambattista, I. A. Aksay and P. G. Debenedetti, *The Journal of Physical Chemistry B*, 2009, **113**, 1438-1446.
14.   K. Koga, G. T. Gao, H. Tanaka and X. C. Zeng, *Nature*, 2001, **412**, 802-805.
15.   S. Abel, F. Sterpone, S. Bandyopadhyay and M. Marchi, *The Journal of Physical Chemistry B*, 2004, **108**, 19458-19466.
16.   K. Bhattacharyya, *Accounts of Chemical Research*, 2003, **36**, 95-101.
17.   H. Hauser, G. Haering, A. Pande and P. L. Luisi, *The Journal of Physical Chemistry*, 1989, **93**, 7869-7876.
18.   L. Klíčová, E. Muchová, P. Šebej, P. Slavíček and P. Klán, *Langmuir*, 2015, **31**, 8284-8293.
19.   N. Nandi and B. Bagchi, *The Journal of Physical Chemistry B*, 1997, **101**, 10954-10961.
20.   R. Biswas, N. Rohman, T. Pradhan and R. Buchner, *The Journal of Physical Chemistry B*, 2008, **112**, 9379-9388.
21.   D. E. Moilanen, E. E. Fenn, D. Wong and M. D. Fayer, *The Journal of Physical Chemistry B*, 2009, **113**, 8560-8568.
22.   V. R. Vasquez, B. C. Williams and O. A. Graeve, *The Journal of Physical Chemistry B*, 2011, **115**, 2979-2987.
23.   T. K. De and A. Maitra, *Advances in Colloid and Interface Science*, 1995, **59**, 95-193.
24.   A. Maitra, *The Journal of Physical Chemistry*, 1984, **88**, 5122-5125.
25.   A. Amararene, M. Gindre, J. Y. Le Huérou, W. Urbach, D. Valdez and M. Waks, *Physical Review E*, 2000, **61**, 682-689.
26.   I. R. Piletic, D. E. Moilanen, D. B. Spry, N. E. Levinger and M. D. Fayer, *The Journal of Physical Chemistry A*, 2006, **110**, 4985-4999.
27.   D. E. Moilanen, E. E. Fenn, D. Wong and M. D. Fayer, *The Journal of Chemical Physics*, 2009, **131**, 014704.

28.   N. Sarkar, K. Das, A. Datta, S. Das and K. Bhattacharyya, *The Journal of Physical Chemistry*, 1996, **100**, 10523-10527.
29.   S. J. Law and M. M. Britton, *Langmuir*, 2012, **28**, 11699-11706.
30.   A. Patra, T. Q. Luong, R. K. Mitra and M. Havenith, *Physical Chemistry Chemical Physics*, 2013, **15**, 930-939.
31.   A. Patra, T. Q. Luong, R. K. Mitra and M. Havenith, *Physical Chemistry Chemical Physics*, 2014, **16**, 12875-12883.
32.   A. A. Bakulin, D. Cringus, P. A. Pieniazek, J. L. Skinner, T. L. C. Jansen and M. S. Pshenichnikov, *The Journal of Physical Chemistry B*, 2013, **117**, 15545-15558.
33.   S. Senapati and M. L. Berkowitz, *The Journal of Chemical Physics*, 2003, **118**, 1937-1944.
34.   C. D. Bruce, S. Senapati, M. L. Berkowitz, L. Perera and M. D. E. Forbes, *The Journal of Physical Chemistry B*, 2002, **106**, 10902-10907.
35.   S. Senapati and A. Chandra, *The Journal of Physical Chemistry B*, 2001, **105**, 5106-5109.
36.   S. Balasubramanian and B. Bagchi, *The Journal of Physical Chemistry B*, 2002, **106**, 3668-3672.
37.   R. Biswas, J. Furtado and B. Bagchi, *The Journal of Chemical Physics*, 2013, **139**, 144906.
38.   J. Chowdhary and B. M. Ladanyi, *The Journal of Physical Chemistry A*, 2011, **115**, 6306-6316.
39.   J. Faeder and B. M. Ladanyi, *The Journal of Physical Chemistry B*, 2000, **104**, 1033-1046.
40.   M. R. Harpham, B. M. Ladanyi and N. E. Levinger, *The Journal of Physical Chemistry B*, 2005, **109**, 16891-16900.
41.   R. Costard, N. E. Levinger, E. T. J. Nibbering and T. Elsaesser, *The Journal of Physical Chemistry B*, 2012, **116**, 5752-5759.
42.   Y. Pang, *Ultrafast Vibrational Dynamics of Water and Confined Water in Reverse Micelles*, ProQuest, 2007.
43.   K. Bhattacharyya and B. Bagchi, *The Journal of Physical Chemistry A*, 2000, **104**, 10603-10613.
44.   T. H. van der Loop, N. Ottosson, S. Lotze, E. Kentzinger, T. Vad, W. F. C. Sager, H. J. Bakker and S. Woutersen, *The Journal of Chemical Physics*, 2014, **141**, 18C535.
45.   P. K. Verma, R. Saha, R. K. Mitra and S. K. Pal, *Soft Matter*, 2010, **6**, 5971-5979.
46.   L. Martinez, R. Andrade, E. G. Birgin and J. M. Martinez, *Journal of computational chemistry*, 2009, **30**, 2157-2164.
47.   R. M. Pashley, P. M. McGuiggan, B. W. Ninham and D. F. Evans, *Science*, 1985, **229**, 1088-1089.
48.   F. Despa and R. S. Berry, *Biophysical Journal*, 2007, **92**, 373-378.
49.   S. Banerjee, R. S. Singh and B. Bagchi, *J Chem Phys*, 2015, **142**, 134505.
50.   E. E. Fenn, D. B. Wong and M. D. Fayer, *Proceedings of the National Academy of Sciences*, 2009, **106**, 15243-15248.
51.   D. E. Moilanen, N. E. Levinger, D. B. Spry and M. D. Fayer, *Journal of the American Chemical Society*, 2007, **129**, 14311-14318.
52.   D. Laage and W. H. Thompson, *The Journal of Chemical Physics*, 2012, **136**, 044513.
53.   F. G. Moore and G. L. Richmond, *Accounts of Chemical Research*, 2008, **41**, 739-748.
54.   K. B. Jinesh and J. W. M. Frenken, *Physical Review Letters*, 2008, **101**, 036101.

55. D. E. Gragson and G. L. Richmond, *The Journal of Physical Chemistry B*, 1998, **102**, 569-576.

56. G. Stirnemann, P. J. Rossky, J. T. Hynes and D. Laage, *Faraday discussions*, 2010, **146**, 263-281; discussion 283-298, 395-401.

57. J. G. Davis, K. P. Gierszal, P. Wang and D. Ben-Amotz, *Nature*, 2012, **491**, 582-585.

58. K. Lum, D. Chandler and J. D. Weeks, *The Journal of Physical Chemistry B*, 1999, **103**, 4570-4577.

59. D. Chandler, *Nature*, 2005, **437**, 640-647.

60. C. S. Tian and Y. R. Shen, *Proceedings of the National Academy of Sciences*, 2009, **106**, 15148-15153.

61. P. Bjelkmar, P. Larsson, M. A. Cuendet, B. Hess and E. Lindahl, *Journal of Chemical Theory and Computation*, 2010, **6**, 459-466.

62. H.-F. Eicke and J. Rehak, *Helvetica Chimica Acta*, 1976, **59**, 2883-2891.

63. M. Zulauf and H. F. Eicke, *The Journal of Physical Chemistry*, 1979, **83**, 480-486.

64. V. R. Hande and S. Chakrabarty, *The Journal of Physical Chemistry B*, 2015, **119**, 11346-11357.

65. J. L. F. Abascal and C. Vega, *The Journal of Chemical Physics*, 2005, **123**, 234505.

66. C. Vega and J. L. F. Abascal, *Physical Chemistry Chemical Physics*, 2011, **13**, 19663-19688.

67. B. Hess, C. Kutzner, D. van der Spoel and E. Lindahl, *Journal of Chemical Theory and Computation*, 2008, **4**, 435-447.

68. G. Bussi, D. Donadio and M. Parrinello, *The Journal of Chemical Physics*, 2007, **126**, 014101.

69. H. J. C. Berendsen, J. P. M. Postma, W. F. van Gunsteren, A. DiNola and J. R. Haak, *The Journal of Chemical Physics*, 1984, **81**, 3684-3690.

70. M. Parrinello and A. Rahman, *Journal of Applied Physics*, 1981, **52**, 7182-7190.

71. B. Guchhait, R. Biswas and P. K. Ghorai, *The Journal of Physical Chemistry B*, 2013, **117**, 3345-3361.

72. M. H. H. Pomata, D. Laria, M. S. Skaf and M. D. Elola, *The Journal of Chemical Physics*, 2008, **129**, 244503.

73. T. Kinugasa, A. Kondo, S. Nishimura, Y. Miyauchi, Y. Nishii, K. Watanabe and H. Takeuchi, *Colloids and Surfaces A: Physicochemical and Engineering Aspects*, 2002, **204**, 193-199.

74. R. Biswas, T. Chakraborti, B. Bagchi and K. G. Ayappa, *The Journal of Chemical Physics*, 2012, **137**, 014515.

75. M. Marchi, F. Sterpone and M. Ceccarelli, *Journal of the American Chemical Society*, 2002, **124**, 6787-6791.

TABLES

Table 1. The number of different species used to simulate the RM and W/O systems. nH_2O, $nAOT$, nNa^+ and $nISO$ are the number of water, AOT, Na^+ counter-ion and isooctane molecules used to build the initial configurations of RMs and W/O systems. The production run lengths for all systems have been shown in the last column.

System	nH_2O	$nAOT$	nNa^+	$nISO$	Production run length (ns)
Bulk water	4125	-	-	-	20
RM w_0= 20	6040	302	302	23474	100
RM w_0=15	2835	189	189	33830	100
RM w_0=10	980	98	98	10111	100
W/O = 20	6040	-	-	5572	20
W/O = 15	2835	-	-	2274	20
W/O = 10	980	-	-	724	20

Table 2. Tri-exponential fitting of orientational time correlation function (OTCF) of water molecules in the I. core region and II. interfacial region of water pools for RM $w_0 = 20, 15, 10$ and W/O = 20, 15, 10 as well as for bulk water. The fitting function is $C_\mu(t) = f_1 \exp\left(-\frac{t}{\tau_1}\right) + f_2 \exp\left(-\frac{t}{\tau_2}\right) + f_3 \exp\left(-\frac{t}{\tau_3}\right)$ where, f_i is the fraction of the i-th component with the timescale being τ_i. The correlation coefficients for the fitting are greater than 0.99 in all cases.

I. For Core Water

System	$\%f_1$	τ_1 (ps)	$\%f_2$	τ_2 (ps)	$\%f_3$	τ_3 (ps)
Bulk water	75	6.16	13	2.26	12	0.14
RM W0 = 20	6	23.84	79	6.04	15	0.47
RM W0 = 15	7	26.56	78	6.03	15	0.46
RM W0 = 10	8	44.82	77	6.25	15	0.40
W/O = 20	59	6.16	27	3.60	14	0.36
W/O = 15	46	6.88	40	4.27	14	0.37
W/O = 10	59	6.84	27	4.10	14	0.37

II. For interfacial water

System	$\%f_1$	τ_1 (ps)	$\%f_2$	τ_2 (ps)	$\%f_3$	τ_3 (ps)
RM W0 = 20	30	99.62	55	6.44	15	0.017
RM W0 = 15	32	97.25	53	6.49	15	0.017
RM W0 = 10	37	104.49	48	6.75	15	0.017
W/O = 20	51	9.25	34	3.74	15	0.017
W/O = 15	55	9.64	30	3.62	15	0.017
W/O = 10	52	10.07	32	4.03	16	0.017

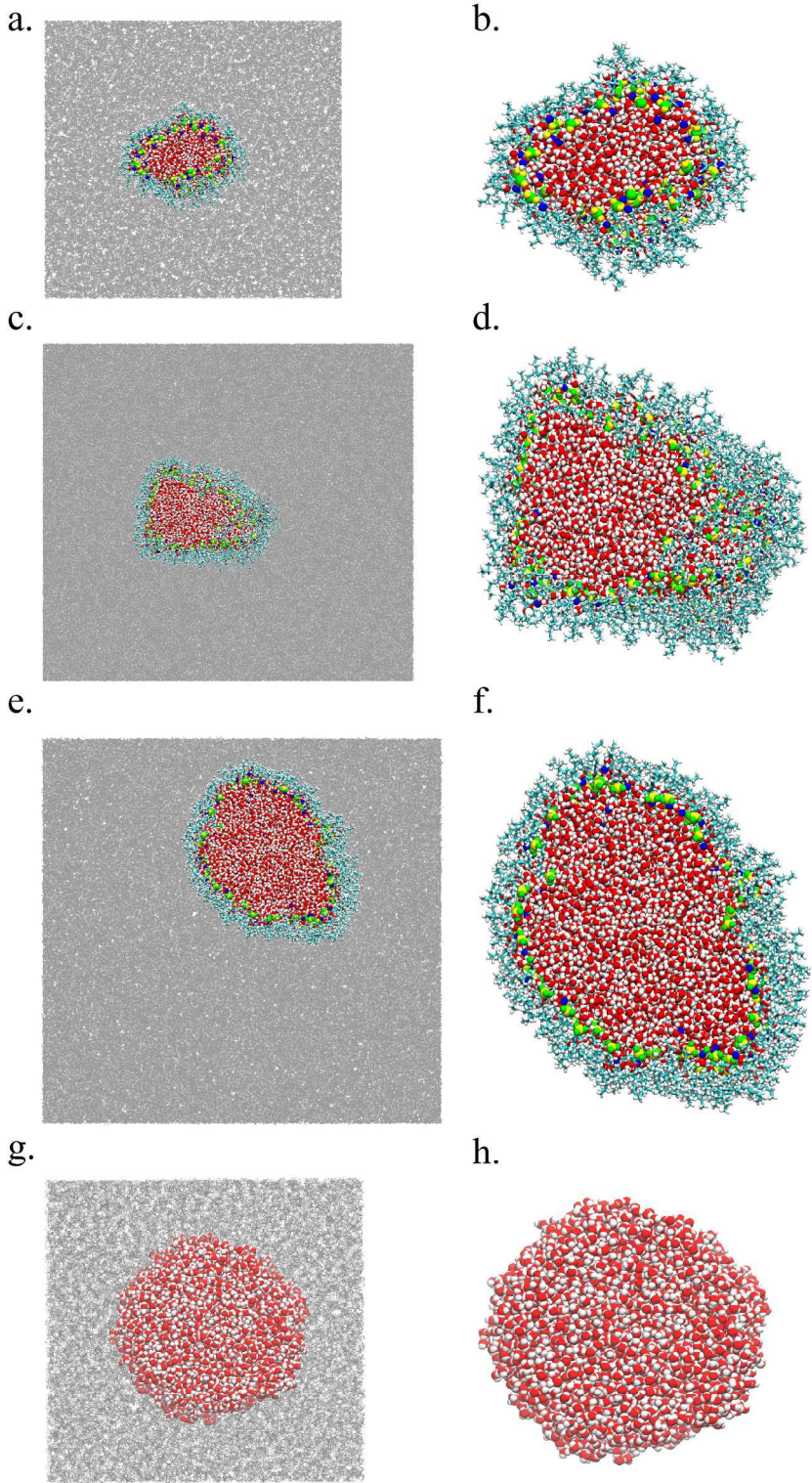**FIGURES**

a.

b.

c.

d.

e.

f.

g.

h.

33

Figure 1: Representative snapshots from the MD simulation trajectories for (a,b) $w_0 = 10$, (c,d) $w_0 = 15$, (e,f) $w_0 = 20$ and (g,h) W/O= 20. The left panel figures show the snapshots with the background isooctane medium included, whereas the right panel figures focus on either the AOT RM system of water pool in W/O system for clarity. The following color scheme has been adopted for various molecular species: isooctane (gray), hydrogen atoms of AOT and water (white), oxygen atoms of AOT head group (green), sulfur (yellow), Na^+ (blue) and remaining oxygen atoms of AOT and water (red). The MD trajectories show large shape fluctuations, particularly for the RM systems, which often adopt non-spherical structures.

Figure 2: Radial profile of shell-wise (a) average number density (ρ), (b) average tetrahedral order parameter (Q), and (c) average dipolar orientation of water molecules with respect to the radial vector as described by $\langle \hat{r} \cdot \hat{\mu} \rangle = \langle \cos \theta \rangle$, where $\hat{r}$ and $\hat{\mu}$ are the unit vectors corresponding to the radial vector (center of mass of water pool to water oxygen) and dipole vector, respectively. All distances are measured from the center of mass of the water pool in respective cases. The dashed and solid lines correspond to the reverse micelle (RM) and water-in-oil (W/O) systems, respectively. The green, blue and red lines represent systems with w_0 or W/O = 10, 15 and 20, respectively.
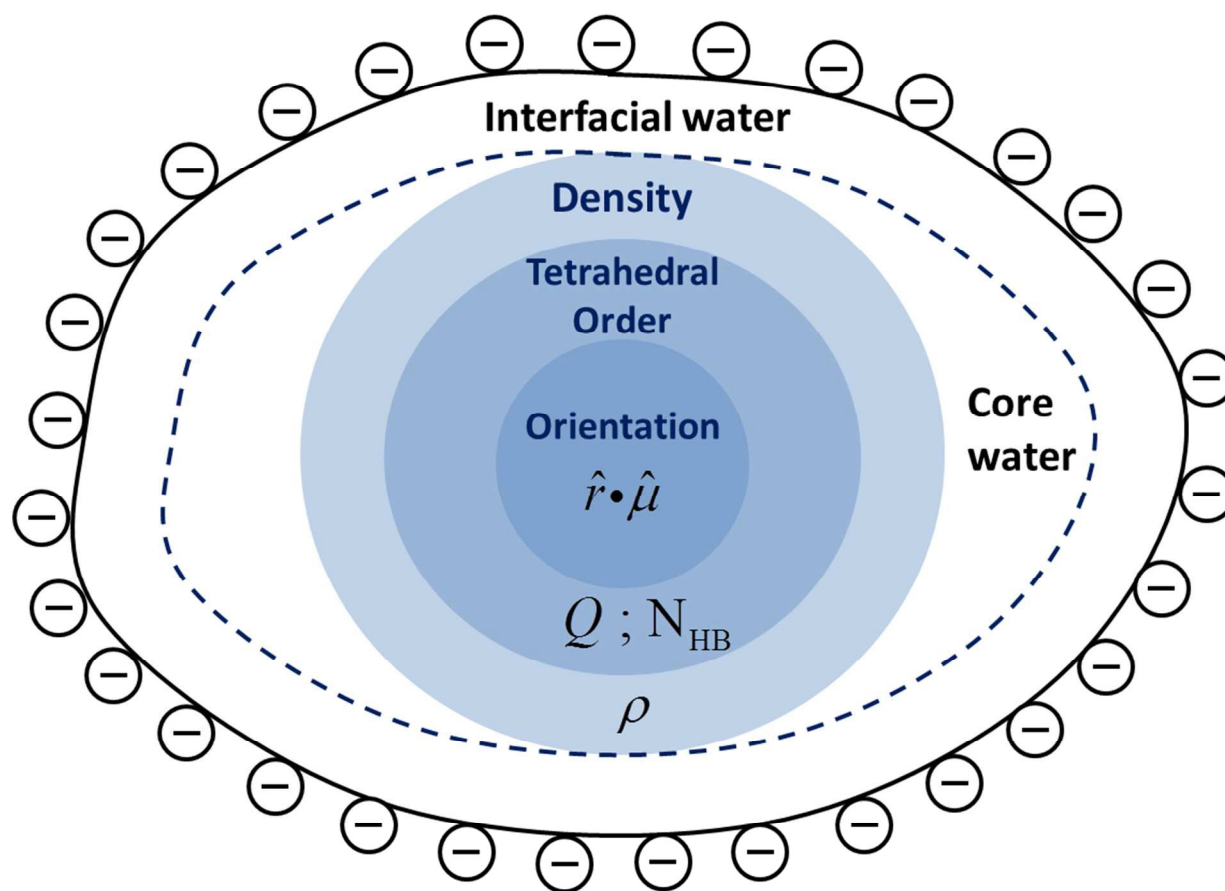
Figure 3. Schematic representation of different regions inside the reverse micelle. The negative

charges around the outermost layer depict the head-groups of the AOT surfactant molecules. We

consider water molecules within 1.1 nm of the charged surface to be the "interfacial water" layer,

where water molecules are expected to have distinct properties as compared to bulk water. Rest

of the water molecules in the interior of the water pool is considered "core water" (inside the

dashed line), which may or may not resemble "bulk water" depending on the property of interest

as shown in Fig.2. The spherical regions provide a visual representation of the size of regions

where bulk-like behavior is recovered for various properties. The effective size of bulk-like

water pool decreases in the order of number density, tetrahedral order parameter (and number of

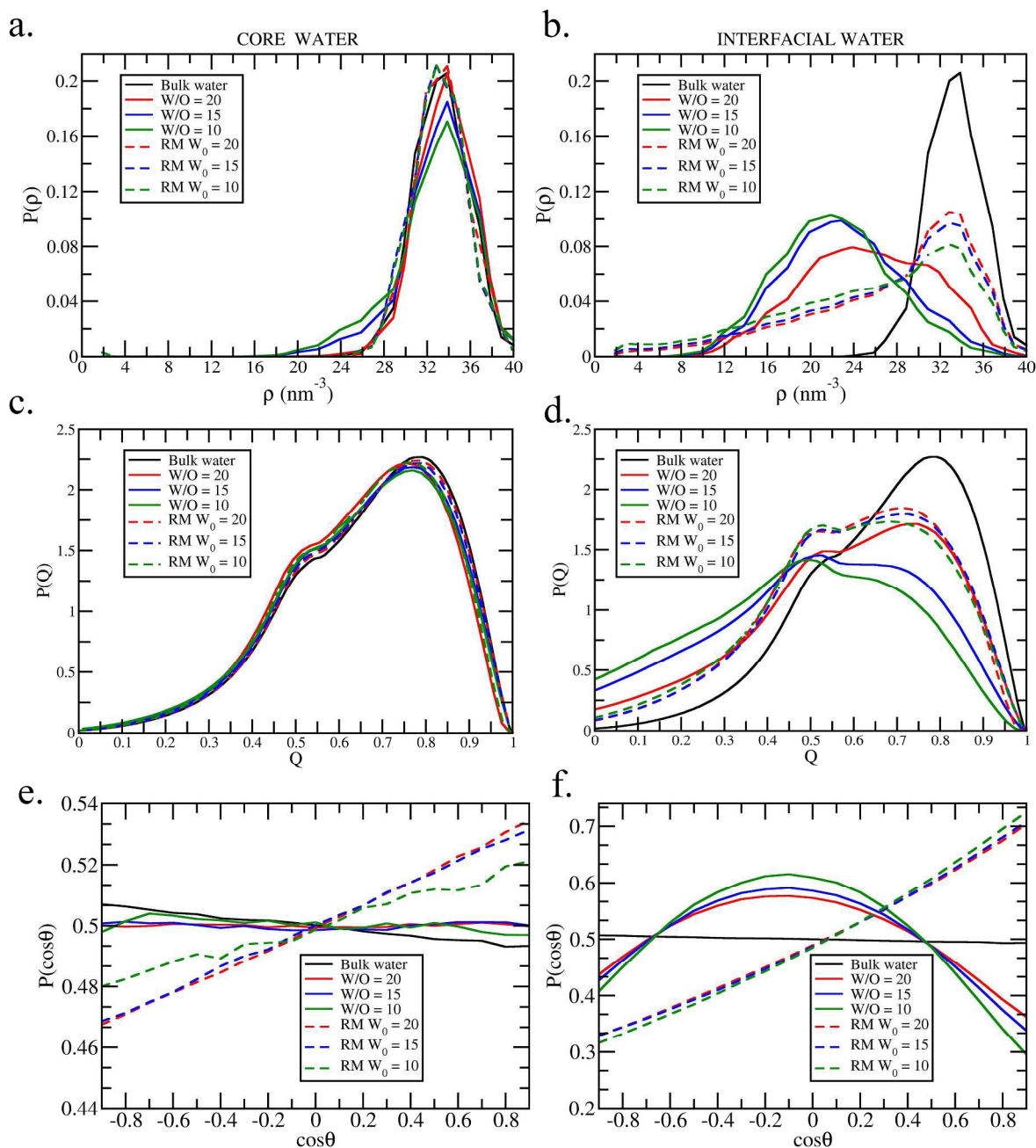hydrogen bond), and average dipolar orientation of water molecules.

Figure 4. Distribution of the structural properties of water for "core water" (left panels) and "interfacial water" (right panels). The top panels (a, b), middle panels (c, d) and bottom panels (e, f) depict the distribution of local number density (ρ), tetrahedral order parameter (Q) and dipolar orientation relative to the radial vector. Here we have combined results for both RM and water-in-oil systems for w_0 = 10, 15 and 20 and compared with bulk water.
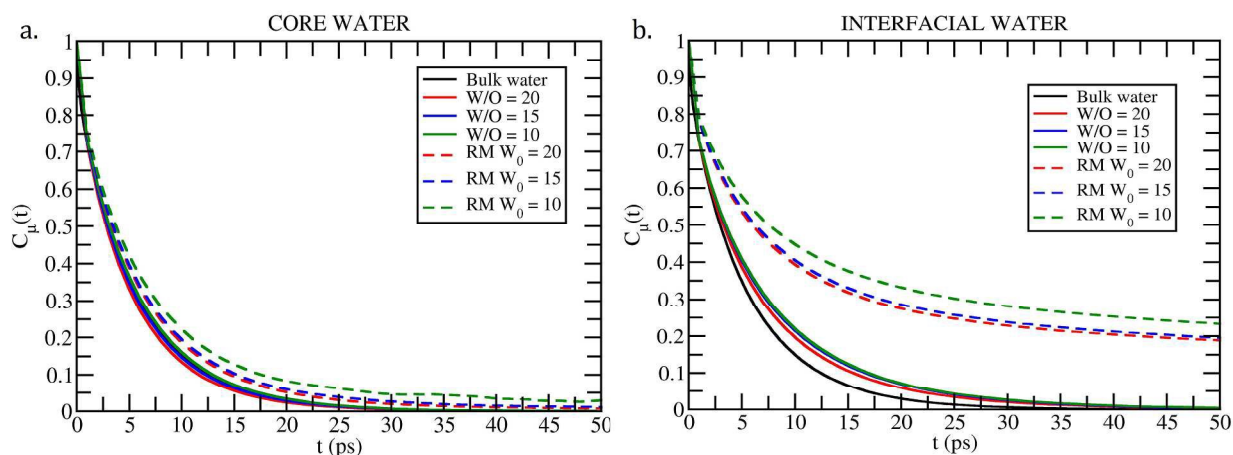
Figure 5. Orientational time correlation function (OTCF) of (a) core water and (b) interfacial water. We compare the OTCF for $w_0 = 10$, 15 and 20 in both RM and water-in-oil systems. The OTCF for bulk water is shown as reference. The OTCF is calculated for the water molecules which continously stay in the respective regions at least for 50ps.
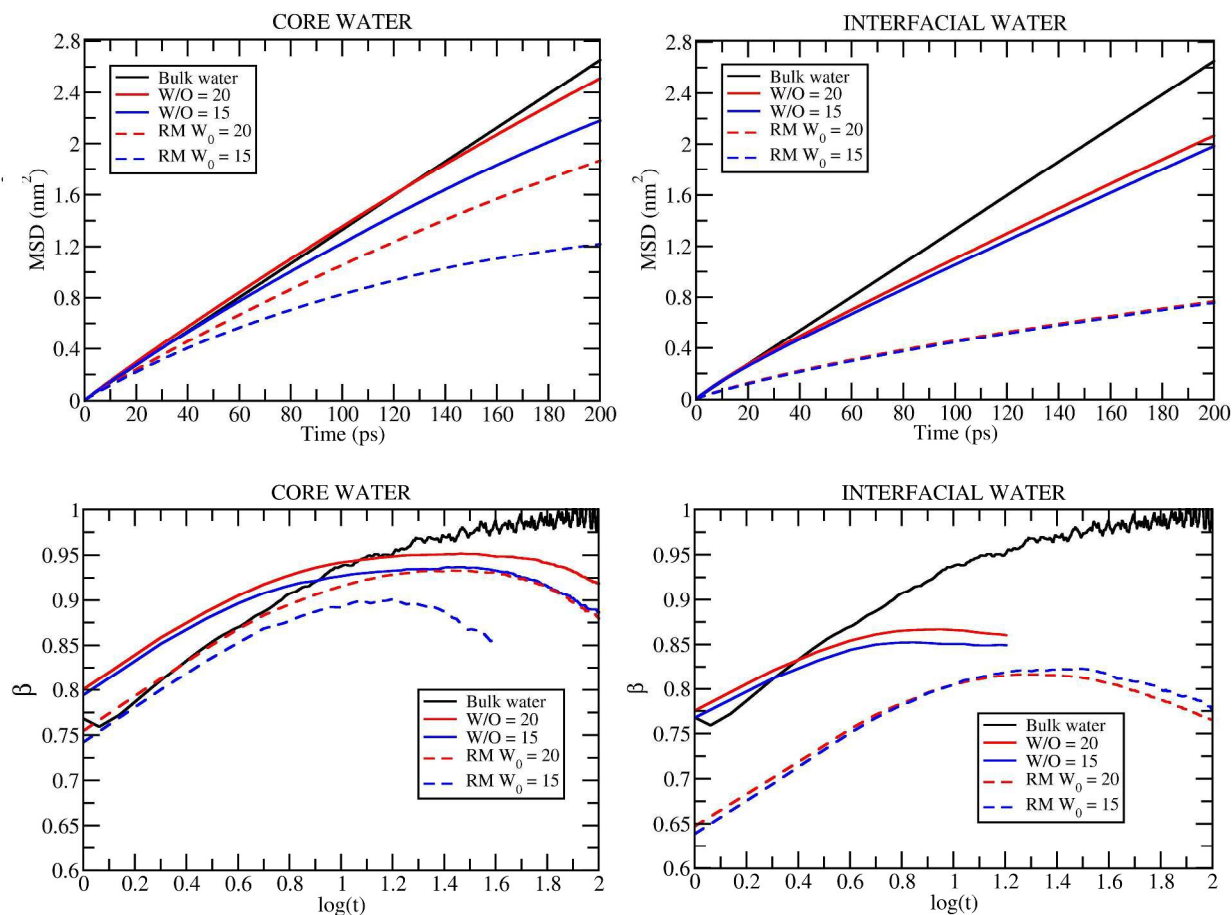
Figure 6. (top panel) Mean square displacement (MSD) versus time for the oxygen atoms of (a) core water and (b) interfacial water molecules. (bottom panel) The slope of the log(MSD) versus log(t), depicting the β exponent, where MSD $r(t) \propto t^\beta$. For a diffusive process, $\beta = 1$, whereas for sub-diffusive process, $\beta < 1$, which seems to be the case for all confined systems studied here. We show the comparison for both RM and water-in-oil systems for $w_0 = 15$ and 20, and compare with the bulk water. MSD is calculated for the water molecules which continously stay in the respective regions at least for 200ps.